A new method for estimating emission ratios in the urban atmosphere: examples of ratios to CO_2, CO and volatile organic compounds in Paris

L. Ammoura[1], I. Xueref-Remy[1], F. Vogel[1], V. Gros[1], A. Baudic[1], B. Bonsang[1], M. Delmotte[1], Y. Té[2], and F. Chevallier[1]

[1]LSCE, Unité mixte CEA-CNRS-UVSQ, UMR 8212, 91191 Gif-Sur-Yvette, France

[2]LERMA, Unité mixte CNRS-ENS-OP-UCP-UPMC, UMR 8112, 75005 Paris, France

Abstract

We propose a new approach to estimate urban emission ratios that takes advantage of the enhanced local urban signal in the atmosphere at low wind speed. We apply it to estimate monthly ratios between CO_2, CO and some VOCs from several atmospheric concentration measurement datasets acquired in the centre of Paris between 2010 and 2014. We find that this approach is little sensitive to the regional background level definition and that, in the case of Paris, it samples all days (weekdays and weekends) and all hours of the day evenly. A large seasonal variability of the $\Delta CO/\Delta CO_2$ ratio in Paris is shown, with a difference of around 60% between the extreme values and a strong anti-correlation (r^2=0.75) with atmospheric temperature. The comparison of the ratios obtained for two short measurement campaigns conducted in two different districts and two different periods (fall and winter) shows differences ranging from -120% to +63%. A comparison with a highly resolved regional emission inventory suggests some spatial variations of the ratio within the city.

1. Introduction

In response to changing air quality and climate, there is a growing interest in quantifying emissions of pollutants and greenhouse gases from urban areas (UNEP 2013, EEA 2014). Urban emissions are usually known through the combination of direct and indirect geospatial energy use statistics with emission factors for individual source sectors. The heterogeneity of the input data in space, time and type makes it difficult to monitor the uncertainties of these inventories. Such monitoring actually receives little incentive at the international level (e.g., Bellassem et al. 2015), but it has been an active topic for scientific research. Some studies have been based on measurement campaigns dedicated to specific sectors, for instance air-composition measurements in road tunnels for traffic emissions

(e.g., Touaty and Bonsang, 2000 ; Ammoura et al., 2014), or in ambient air for power plants (Zhanga and Schreifels, 2011), waste water treatment plants (Yoshida et al., 2014 ; Yver-Kwok et al. 2015) or for the overall city-scale emissions (Lopez et al., 2013; Turnbull et al., 2011, 2015). Measurements made in the ambient air are affected by dilution in the atmospheric boundary layer, but this effect cancels out for mole fraction ratios between the considered species. The mole fraction ratios estimated from ambient air can also be directly interpreted in terms of emission ratios provided that the measured molecules share the same origin. Ultimately emission ratios may be interpreted in terms of sectoral emissions. In practice, the mixing of air parcels of various origins and ages largely hampers the interpretation. To isolate the local urban signal, measurements for species with a significant life time in the atmosphere have to be corrected from background influence, usually based on other measurements made in the free troposphere or at a remote site (e.g., Lopez et al. 2013; Turnbull et al, 2015). Isotopic measurements, like those of $^{14}CO_2$, can also allow better focusing the analysis on anthropogenic activities (e.g., Levin and Karstens, 2007; Turnbull et al., 2011). Last, atmospheric transport models are used in a few studies to quantify the contributions of the different sources within an inverse modelling approach (e.g., Saide et al. 2011, Lauvaux et al., 2013; Bréon et al. 2015).

Here, we investigate the possibility of benefiting from an enhanced local urban signal at low wind speed for estimating emission ratios from atmospheric composition measurements. Indeed, when the atmosphere is not well ventilated, emission plumes get trapped in the atmospheric boundary layer close to their origin. The resulting large peaks in mole fractions time-series are easily visible compared to typical background variations. In this manuscript, we make the first attempt to fully exploit this well understood behaviour. We use several measurement campaigns of CO_2, CO and Volatile Organic Compounds (VOCs) performed in Paris in 2010, 2013 and 2014 to validate the approach and to evaluate local emissions ratios. Paris is the third largest megacity in Europe and the largest one in France. It comprises around 12 million people when including its suburbs. The population density is one of the highest in Europe with 21347 inhabitants per km² (INSEE, 2014). According to the latest Paris inventory of Airparif (Association in charge of monitoring the air quality in the Paris region) provided for year 2010, emissions of CO_2 are mainly from the traffic (29%) and residential and service sectors (43%) (Airparif, 2013). Airparif also estimated VOC emissions and their main origins are the same as those of CO_2 (such as traffic or residential heating).

The paper is structured as follows. Section 2 presents the measurements and the data. Section 3 starts with a presentation of typical measurements and a discussion about the choice of the background level, presenting two different options. The analysis method itself developed to estimate urban emission ratios is described in Section 3.3 including sensitivity tests (Sections 3.3.2 and 3.3.3). Section 4 presents the results obtained for different periods of the year and different years. Section 4.1 gives the interpretation of the ratios determined with our method and discusses the representativeness of these ratios. Section 4.2 presents the seasonal variability of the $\Delta CO/\Delta CO_2$ ratio in Paris and Section 4.3

compares all ratios between co-emitted species obtained during two short campaigns in Paris.

2. Methods

2.1 Site description

All atmospheric composition measurements presented in this study have been made in the centre of Paris. The instruments were installed at two sites. The first one is located on the Jussieu campus of University Pierre et Marie Curie (UPMC) at the QualAir station (http://qualair.aero.jussieu.fr). This station stands on the roof of a building, on the left bank of the river Seine (48°50'N, 2°21'E and 23 m above ground level). A botanical garden of 28 hectares, the Jardin des Plantes, lies about 500 m from the measurement site. The closest motorways are about 4 km on the south and on the south-east, but the university is surrounded by many streets which are particularly congested during rush hours. The emission activities in the centre of Paris essentially originate from road traffic activities and from the residential and service sectors, since most industrial activities have been removed in the 1960s (AIRPARIF, 2013).

The second measurement site is the roof of Laboratoire d'Hygiène de la Ville de Paris (LHVP) located about 2 km from the Jussieu campus, south-east of it (48°49'N and 2°21'E and 15 m above ground level). It dominates a public garden of 4.3 hectares, the Parc de Choisy. Residential buildings and arterial roads also surround this site. The closest motorway is a few hundred meters south of the site.

2.2 Instrumentation and air sampling

2.2.1 Joined MEGAPOLI/CO_2-Megaparis winter campaign

Our first campaign was performed jointly within the MEGAPOLI European project (Megacities: Emissions, urban, regional and Global Atmospheric POLlution and climate effects, and Integrated tools for assessment and mitigation project, http://megapoli.info/) and the CO2-Megaparis project (https://co2-megaparis.lsce.ipsl.fr). This 'winter campaign' took place in Paris during January-February 2010 (Dolgorouky et al. 2012, Lopez et al. 2013).

Two instruments were deployed at the LHVP. A Gas Chromatograph equipped with a Flame Ionisation Detector (GC-FID, Chromatotec) sampled Non-Methane Hydrocarbons (NMHCs). Mole fractions of alkanes, alkenes, alkynes and aromatic compounds were obtained with a time resolution of 30 minutes (air is sampled during the first 10 minutes and analysed during the next 20 minutes). More details can be found in Gros et al. (2011) and Dolgorouky et al. (2012).

A Cavity Ring-Down Spectrometer (CRDS G1302, Picarro Inc) was also deployed to analyse CO_2, CO and H_2O mole fractions with a time resolution of 1 s (see Lopez et al., 2013, for more details).

2.2.2 Long-term continuous CO_2 and CO measurements

A Cavity ring-Down analyser (CRDS G1302, Picarro Inc.) performed continuous CO_2, CO and H_2O measurements in Jussieu continuously from 4 February 2013 to 11 June 2014 with a time resolution of 1 s. This instrument was calibrated about every two months using three 40 L aluminium gas tanks. These cylinders were previously calibrated for CO_2 and CO dry air mole fractions against the NOAA-X2007 scale for CO_2 and the NOAA-X2004 for CO. A fourth gas cylinder was used as a target to evaluate the repeatability of the data and the drift of the instrument. This target was analysed for 20 minutes every 12 h between 4 February 2013 and 25 August 2013 and for 15 minutes every 47 h since 26 August 2013. Using the target gas measurements, we estimate the repeatability and the trueness (closeness of agreement between the average of a huge number of replicated measured species concentrations and a reference concentration, BIPM (2012)) of the 1 minute averaged data to be, respectively, 0.05 ppm and 0.03 ppm for CO_2 and 6.8 ppb and 3.7 ppb for CO.

2.2.3 'Multi-CO_2' field-campaign

Several instruments were installed next to the CRDS analyser in Jussieu from 11 October 2013 until 22 November 2013 within the Multi-CO_2 project.

For the compounds of interest for this study (CO_2, CO and light VOCs), the same instruments that were used during the joined MEGAPOLI/CO_2-Megaparis campaign were deployed (see Section 2.2.1). VOC mole fractions were measured using a gas chromatograph (Chromatotec) calibrated against a reference standard (National Physics Laboratory, Teddington, UK). Some VOCs were selected for this study because they share the same origins (such as traffic or residential heating) than other VOCs, CO and CO_2: ethane, ethylene, acetylene, propane, propene, i-pentane and n-pentane. The total uncertainty of the data was estimated to be better than 15%.

Meteorological parameters (wind speed and direction, temperature) were also monitored (instrument WMR2000, OREGON Scientific).

2.3 Data processing

As the time resolution was different for both instruments (CRDS and GC-FID), the data have been synchronized. The chosen time interval was the one imposed by GC-FID measurements. Data from GC-FID were acquired for 10 minutes every 30 minutes, the given time stamp corresponding to the beginning of the measurement. Thus for each compound measured by the other instruments (CRDS and meteorological instruments), data have been averaged on the same 10 minutes interval. Finally, in this study, all the data have a same time step of 30 minutes.

3. Results

3.1 Typical time series and identification of specific meteorological events

Figure 1 shows an example of atmospheric gas dry air mole fractions time series collected during the Multi-CO_2 campaign in 2013, with a time step of 30 min. The wind speed during the same period is also represented on the figure (1e). Time series recorded during the joined MEGAPOLI/CO_2-Megaparis campaign in 2010, as well as the continuous measurements of CO_2 and CO in Jussieu are shown in the supplementary material.

Mole fractions of the different species appear to co-vary much, despite the different lifetime of the species: CO_2 and CO have typical life time in the atmosphere (τ) much longer than the observation period whereas acetylene has a τ of a 13 days and ethylene has a τ of a few hours. In comparison, the meteorological events in Paris during the campaign lasted from a few hours to one day so that VOCs with a τ longer than two days, like acetylene, can be almost considered as non-reactive species. For shorter-lived species, here only ethylene and propene (1 day > τ > 5 hours), we computed the correlations between these species and acetylene. When considering all the data of the Multi-CO_2 campaign (without any selection), coefficients of determination are high (r^2>0.70). These tight correlations between VOCs with different reactivity suggest a limited impact of the chemistry.

In Figure 1, we identify some events when the mole fractions of all species were significantly higher than elsewhere over the campaign duration (1.25 to 6 times as high). These periods (30 and 31 October, 10 and 11 November) appear to be systematically linked to specific meteorological conditions when the wind speed was very low (less than 1 $m.s^{-1}$). The mole fractions obviously increased as the result of the stagnation of local emissions in the atmosphere. However, three periods with low wind speed do not correspond to significant peaks in mole fractions (on 5, 6 and 7 November 2013). These 3 periods were too short (they last around 2h) for the accumulation of emissions in the atmosphere to have taken place and did not result in high mole fractions. There is one more period that we can highlight and for which the wind speed was less than 1 $m.s^{-1}$, from 17 November 15:00 (UTC) to 18 November 7:00 (UTC). The mole fractions were higher than the common baseline due

to changes in synoptic conditions. However, no significant peaks are visible. We notice that during this period, even though the wind speed was low, wind came from one sector only (from 90 to 190°) whereas there is no specific wind direction associated to the large peaks of the other periods (turning wind, see Figure 2 (a)). In the case of a dominant wind direction, and despite low wind speeds, emissions did not seem to have accumulated in the atmosphere (there may have been slowly evacuated). The wind roses in the two different cases are represented in Figure 2. To summarise, periods with low wind speed and non-directional winds are the focus of the present study because they show a distinct local emission signal in the mole fractions.

3.2 Background levels

The previous data selection does not remove all influence of long-range transport (advection) and dispersion in the measurements and there is still a need to remove a background level, especially in the case of species with significant lifetime in the atmosphere like CO_2. Most of the previous studies whose main interest was CO_2 defined a continental clear-air background to correct the CO_2 data. For example, data from Mace Head in Ireland (Lopez et al., 2013) or from Jungfraujoch in Switzerland (Vogel et al., 2010) are often considered as background data for measurements in Europe, but strictly speaking they are too far from Paris to isolate the city signal. Measurements in the free troposphere have also been used as a baseline (Miller et al., 2012; Turnbull et al., 2011), but are particularly expensive to make and are not available for our study period. For short-lived species, the definition of the background is not as critical and the smallest measured value is often used.

Here, we investigate two options to define the urban background levels. The first option takes advantage of the fact that the urban emissions are positive fluxes, i.e. which increase local atmospheric mole fractions. We define background mole fractions as all measurements smaller than the fifth percentile of the species over a moving window. The moving window allows accounting for the dependence of the background on the synoptic situation or on the time of year, as the background changes seasonally for many gases. As the average characteristic time of synoptic changes is a few days, and in order to gather a significant amount of data, we define overlapping windows of three days that start every day at 00:00 (UTC), in increments of 1 day. Figure 1 displays the selected lowest 5% as black disks for some species measured during the Multi-CO_2 campaign. In order to avoid discontinuities, we linearly interpolate the selected data to obtain a background mole fraction time series with a time resolution of 30 minutes (black curves on Figure 1).

This background definition is simple to implement because it does not require additional measurements. Furthermore, it accounts for different wind sectors. We noticed a difference of 8 ppm between continental (0-180°) and oceanic (180-360°) sectors for the averaged CO_2 background derived from the 5^{th} percentile calculation. This background

219 definition is expected to work well for all species that do not have local sinks in the
220 atmosphere or at the surface. We saw in Section 3.1 that chemical sinks could be neglected
221 for our measurements, but in the case of CO_2 during the vegetation-uptake season (summer
222 in particular), vegetation within Paris also contributes to populating the fifth percentile.

223 Our second option (for CO_2 only) defines the background from a publicly available
224 analysis of the global atmospheric composition. We test it for CO_2, the species for which the
225 first definition may be the least appropriate. The definition of the background level of CO_2
226 relies on the global inversion product of the Monitoring Atmospheric Composition and
227 Climate project (MACC v13.1, http://www.copernicus-atmosphere.eu/, Chevallier et al.,
228 2010). This product has a resolution of $3.75^o \times 1.9^o$ (longitude-latitude) in space and of 3 h in
229 time. It combines the information from 131 CO_2 stations over the globe and a transport
230 model within a Bayesian framework and estimates the CO_2 surface fluxes over the globe
231 together with the full 4D CO_2 field.

232 We extracted the 3-hourly time series of the CO_2 concentrations from the MACC
233 database for the eight grid points that surround our two measurement sites, Jussieu and the
234 LHVP. The CO_2 background mole fraction is estimated as the linear interpolation in time of
235 the analysed CO_2 concentrations averaged over the eight grid points. In the following, we call
236 *Δspecies*, the mole fractions excess from the background as defined by either method.

237 A comparison of the results obtained using the two background definitions
238 successively is presented in Section 3.3.3.

239

240 **3.3 Determination of the ratios between co-emitted species**

241 **3.3.1 Description of the method**

242 We present next the method to evaluate ratios of excess mole fractions between 2
243 species ($\Delta species_1$ and $\Delta species_2$). We consider a moving window of 4 h in increments of 30
244 minutes (each period contains 8 points). On each period, we compute the coefficient of
245 determination r^2 between $\Delta species_1$ and $\Delta species_2$ and use a linear regression to evaluate
246 the slope (type II model regression in which errors on both axes are accounted for). This
247 slope defines a ratio between the two considered Δspecies over the 4h period. We also
248 calculate the difference between maximum and minimum $\Delta species_1$, which is plotted on the
249 *x* axis, over this period (we name it $\delta\Delta species_1$). The motivation for this amplitude
250 computation will be developed in Section 4.1. These calculations are made if more than 5
251 points exist during the time period and if species excesses are linearly related (a *p*-value test
252 relative to linear relationship of species excesses is conducted and *p*-value<0.001 are
253 selected). As an example, on a 4h period, we compute (i) the coefficient of determination r^2
254 between ΔCO and ΔCO_2, (ii) the slope, which well fits the considered dataset (thus giving the
255 $\Delta CO/ \Delta CO_2$ ratio over this period) and (iii) $\delta\Delta CO_2$.

In Figure 3, we show some examples of ratios determined on each 4h period against the local corresponding species offset $\delta\Delta CO_2$. They have a simple structure with a horizontal asymptote when $\delta\Delta CO_2$ is high. The equation of the asymptote defines the average ratio. Interpretation and representativeness of this ratio are discussed in Section 4.1.

In order to unambiguously define the equation of this horizontal asymptote, and the related value of the ratio, we apply a filter on r^2 and on $\delta\Delta species_1$ that isolates the asymptote. We apply this criterion to measurements spread over a month. The sensitivity of the ratios to all tested criteria is presented in Section 3.3.2. The final choice of a criterion is a compromise between a cautious selection of points (derived from the criterion on r^2 and $\delta\Delta species_1$) to clearly extract the local-signal asymptote, and a selection of enough points to get a robust ratio. Finally, the equation of the horizontal asymptote is the ratio (we impose a slope of zero). The ratio uncertainty is computed at a confidence level of 68% (1-σ).

3.3.2 Sensitivity to the criterion on r^2 and $\delta\Delta CO_2$

We present here a sensitivity test for the criterion on r^2 and $\delta\Delta CO_2$ in the case of the $\Delta CO/\Delta CO_2$ ratio during the Multi-CO_2 campaign. We evaluate this ratio using the method described in Section 3.3.1 and vary the thresholds on r^2 (with values 0.6, 0.7, 0.8 and 0.9) and on $\delta\Delta CO_2$ (with values 15, 20, 25, 30, 35 and 40 ppm).

Considering a given r^2 ($\delta\Delta CO_2$ can vary and be higher than 15, 20, 25, 30, 35 or 40 ppm), we find less than 10% difference between all the derived ratios. For the other case, considering a fixed $\delta\Delta CO_2$ offset and a varying r^2, differences between all ratios were found to be less than 6%. However, tighter restrictions on the criterion result in fewer available data points that sample the emission conditions within the month less well. As an example, for the couple (r^2>0.6, $\delta\Delta CO_2$>15ppm), 211 points are selected in the asymptote whereas for the one (r^2>0.9, $\delta\Delta CO_2$>30ppm), only 39 points remain. We choose the criterion r^2>0.8 and $\delta\Delta CO_2$>20ppm to determine the $\Delta CO/\Delta CO_2$ ratio during the Multi-CO_2 campaign: it keeps more than a hundred points to define the asymptote. The same test was conducted on all studied ratios and differences between derived ratios do not exceed 10%, which is lower than the 15% error imposed by the uncertainty on VOC data. The data selection for several ratios, including $\Delta CO/\Delta CO_2$, is presented on Figure 3.

3.3.3 Sensitivity to the background choice

In this section, we test the influence of the chosen background definition on the obtained $\Delta CO/\Delta CO_2$ ratio using the methods described in Section 3.3.1. We compare $\Delta CO/\Delta CO_2$ ratios for 2013 using the 5^{th} percentile or MACC simulations as background levels (MACC simulations for 2014 were not available when this study was conducted). The

evolution of the ratios for both options is presented in Figure 4. We evaluate the relative difference between the ratios derived from the two options (in % of the ratio obtained with the fifth percentile as background). Differences vary from -17% in August 2013 to +11% in September 2013. The highest differences are found for the summer months (11% on average), and the lowest ones for the winter months (3.2% on average). These results show that the definition of the background does not significantly affect the derived ratios, even during the summer months. This comes from the fact that urban mole fractions during low wind speed periods are usually larger enough than the background mole fractions (from around 1.25 to 6 times more).

After these analyses, we finally choose to define background levels using the fifth percentile on a running window of 3 days as described in Section 3.2.1. However, tests were conducted using the tenth percentile (and a running window of 3 days) or changing the length of the running window between 1 and 5 days (but still considering the fifth percentile). No significant difference was found using the tenth percentile (less than 2% difference between the two derived $\Delta CO/\ \Delta CO_2$ ratios). Comparing $\Delta CO/\ \Delta CO_2$ ratios obtained with different lengths of the running window, ratios differ by less than 6% from one case to another, thus consolidating our choice for background levels.

4. Discussion

We apply the method presented in Section 3.3.1 to assess ratios between co-emitted species in Paris. In this section, we first discuss the interpretation and the representativeness of the ratios determined using the method previously presented. Then, we divide the analysis in two parts. First we focus on the seasonal variability of the $\Delta CO/\ \Delta CO_2$ ratio using continuous measurements acquired from February 2013 to June 2014. Then we compare the ratios between co-emitted species and CO_2 obtained for the two short campaigns (in Section 4.3).

4.1 Interpretation and representativeness of the ratios determined with the asymptotic method

The *x* axis in Fig. 3 ($\delta\Delta species_1$) represents the variability of the species excess over a 4h-period. Large values correspond to a strong increase or decrease in the species local emissions, and highlight the concentration peaks that occur at low wind speed. The presence of an asymptotic value in the monthly ratio plots like that of Fig. 3 suggests that the ratios do not vary much within the month. This stability is also confirmed by the regular spread of the selected events throughout the month. For instance, applying our method to the continuous CO and CO_2 measurements acquired in 2013/2014 in Paris, we notice that all days (weekdays and weekends) and all hours of the day were sampled equally: no period type is

systematically missing (see Figure 4). This feature allows our method to yield a robust average ratio per month in Paris.

4.2 Seasonal variability of the $\Delta CO/ \Delta CO_2$ ratio in Paris

The evolution of the $\Delta CO/ \Delta CO_2$ ratios in Jussieu between March 2013 and May 2014 is presented in Figure 5. It shows a large seasonal variability with a maximum value in winter and a minimum value in summer. There is a difference of around 60% between these extreme values (minimum value: 3.01 ppb/ppm, maximum value: 6.80 ppb/ppm).

Given the large seasonal cycle observed, we hypothesise that temperature is an important driver of the $\Delta CO/ \Delta CO_2$ ratio. The monthly atmospheric temperature measured during the low wind speed periods is also shown in Figure 5. The two curves are much anti-correlated (r^2=0.75): when the temperature is high, the ratio is low - and reciprocally. This is likely the consequence of higher emissions when temperatures are low because residential heating is important whereas in summer, when temperatures are high, emissions mainly come from traffic, residential cooking and service sectors which all together seem to correspond to a lower $\Delta CO/ \Delta CO_2$ ratio. The difference in emissions between the two extreme seasons relies on the importance of residential heating use. The differences in the ratios may indicate that higher ratios are observed for residential heating than for other sources. This is not in agreement with data from the Airparif inventory: the annual CO/CO_2 for residential heating and for the other sectors are respectively 2.7 ppb/ppm and 7.1 ppb/ppm. This is in accordance with spatialised European emission inventories (Vogel et al., 2013). However, we cannot exclude the impact of other drivers such as traffic as several studies previously showed that CO emissions are more important when vehicles work at lower temperature than the optimal value (Ammoura et al., 2014; SETRA, 2009). However, to our best knowledge, no study characterised the link between vehicle emissions and ambient temperature.

The Airparif inventory does not seem to show a seasonal variability as there is almost no difference on CO/CO_2 ratios between winter and summer: 3.1 ppb/ppm in January against 3.6 ppb/ppm in August. The comparison between these estimates and our observations suggests the possible influence of another source. Indeed, wood burning is a major part of CO emissions from the residential sector (around 90%) but is not taken into account in Airparif CO_2 emissions because it is referenced as biomass burning (and is thus not an anthropogenic component). The differences may be adjusted accounting for this source also for CO_2 emissions and may explain that there is no seasonal variability in the Airparif inventory. However, we were not able to evaluate this point in our study.

4.3 Emission ratios in Paris: Multi-CO_2 vs MEGAPOLI/CO_2-Megaparis

The ratios between the co-emitted species for the Multi-CO_2 campaign, derived from our method, are presented in Table 1. The ones for the MEGAPOLI/CO_2-Megaparis campaign are reported in the supplementary material.

Generally, ratios are different between the two campaigns. We notice differences from -120% to +63%. A satisfactory agreement is found between the two campaigns for the ratios that are reported in bold in Table 1 (less than 15% of difference). Several explanations can be given for these differences. First, measurements were not carried out in the same year: 2010 for the joined MEGAPOLI-CO_2-Megaparis campaign and 2013 for the Multi-CO_2 one. The differences in the ratios may illustrate some evolution in the emission structure (as an example, some technological improvements can occur for vehicles or heating systems). Secondly, these differences may highlight the importance of the seasonal variability of the ratios, which was shown in Section 4.2. Indeed, measurements were performed in autumn (October-November) for the Multi-CO_2 campaign and in winter (January-February) for the MEGAPOLI/CO_2-Megaparis one. The $\Delta CO/\Delta CO_2$ ratio from the latter campaign is also reported in Figure 5 for the corresponding month of the year: it aligns well on the seasonal variability observed in Jussieu, even though this campaign was made four years before. Furthermore, average temperatures during the low wind speed periods were not the same: 10°C during the Multi-CO_2 campaign, 3°C during the MEGAPOLI/CO_2-Megaparis one. This is in agreement with the argument developed in Section 4.2: residential heating is more important in the heart of winter and its emissions make the $\Delta CO/\Delta CO_2$ ratio higher. Finally the instruments were not installed at the same location in the centre of Paris (there are 2 km between the two locations). Thus the emission area of influence could be different because the local activities are not exactly the same around the two sites. As an example, highways, where the vehicle speed is limited to 80 $km.h^{-1}$ and the vehicle flow is high, are closer to the LHVP (MEGAPOLI/CO_2-Megaparis measurements), leading this site to be more influenced by large traffic emissions. This spatial variability of the ratios in Paris is confirmed by the latest Paris emission inventory Airparif 2010. Airparif provides annual CO and CO_2 emissions by districts in Paris. Jussieu is in the 5^{th} district and the LHVP in the 13^{th}. According to the latest Airparif inventory, the annual CO/CO_2 ratios are respectively 2.43 ppb/ppm and 3.74 ppb/ppm for the 5^{th} and the 13^{th} districts. However, the good agreement between the ratio from the MEGAPOLI/CO_2-Megaparis campaign (measurements in 2010) and the one derived in Jussieu (measurements in 2014) indicates that the seasonal variability is the main driver for the evolution of the ratios.

5. Conclusion

We have investigated the possibility to characterise local urban emissions through atmospheric mole fraction measurements collected during low wind speed periods. In the

case of Paris, we have shown that this approach significantly reduces the sensitivity of the results to the species background level definition, even in the case of CO_2. Thanks to long-term continuous measurements, we have also shown that the low wind speed conditions in the centre of Paris (especially in Jussieu) sample the hours of the day and the days of the week rather evenly, so that the method characterises an average urban atmosphere.

The comparison of ratios obtained for the two measurement campaigns, Multi-CO_2 and MEGAPOLI/CO_2-Megaparis, shows differences from -120% to +63% for 9 atmospheric species. Such differences may reveal spatial and seasonal variability in the ratios because the two campaigns took place at different sites, during different years and seasons. However, the evolution of the ratios seems to be mainly influenced by the seasonal changes. This seasonal variability was assessed for the CO to CO_2 ratios for the period from February 2013 to June 2014, showing a strong anti-correlation with monthly atmospheric temperature, likely linked to seasonal changes in emissions sources (for example, domestic heating is predominant in winter and non-existent in summer). We provide evidence on the importance of residential heating in the total $\Delta CO/ \Delta CO_2$ ratio. This ratio is higher than the ones for other sectors which is in contradiction to current estimates from the Airparif inventory.

The determination of these average ratios may be useful to assess the estimates provided by emission inventories. Indeed, city-scale emission inventories mainly focus on air quality, and the link with greenhouse gases, especially with CO_2, is not well made. The combination of the well-known total pollutant emissions with the ratios estimated by our experimental approach should allow a better quantification of total CO_2 emissions.

Acknowledgements:

We acknowledge IPSL (Institut Pierre Simon Laplace) for funding the Multi-CO_2 project as well as the Ville de Paris for funding the project entitled *Le CO_2 parisien* which allowed us to carry out the measurement campaign. We are very grateful to Pascal Jesek from LERMA for his technical support in Jussieu and to Christof Janssen for this fruitful collaboration. We thank AIRPARIF and particularly Olivier Perrussel for the latest Aiparif inventory and the productive discussions. We are also very grateful Dominique Baisnee, Nicolas Bonnaire and Roland Sarda-Estève for their technical help during the Multi-CO_2 campaign. We acknowledge François Ravetta for the access to the QUALAIR platform. We thank Julie Helle for her technical help. We thank the ICOS-Ramces team for the calibration of the gas tanks to the WMO NOAA scale as well as François Truong and Cyrille Vuillemin for their precious technical advices. We acknowledge the Megapoli and CO_2-Megaparis projects for providing support to this study. This work was also partly supported by CNRS, CEA and UVSQ.

441 **References**

442 AIRPARIF, Bilan des émissions de polluants atmosphériques et de gaz à effet de serre en Île-
443 de-France pour l'année 2010 et historique 2000/2005 : Méthodologie et résultats, Juillet
444 2013.

445 Ammoura, L., Xueref-Remy, I., Gros, V., Baudic, A., Bonsang, B., Petit, J.-E., Perrussel, O.,
446 Bonnaire, N., Sciare, J., and Chevallier, F.: Atmospheric measurements of ratios between
447 CO_2 and co-emitted species from traffic: a tunnel study in the Paris megacity, Atmos. Chem.
448 Phys., 14, 12871-12882, doi:10.5194/acp-14-12871-2014, 2014.

449 Bellassen, V. and Stephan, N.: Accounting for Carbon : Monitoring, Reporting and Verifying
450 Emissions in the Climate Economy, Cambridge University Press, Cambridge, UK, 2015.

451 Borbon, A., Gilman, J. B., Kuster, W. C., Grand, N., Chevaillier, S., Colomb, A., Dolgorouky,
452 C., Gros, V., Lopez, M., Sarda-Esteve, R., Holloway, J., Stutz, J., Petetin, H., McKeen, S.,
453 Beekmann, M., Warneke, C., Parrish, D. D., and de Gouw, J. A.: Emission ratios of
454 anthropogenic volatile organic compounds in northern mid-latitude megacities:
455 Observations versus emission inventories in Los Angeles and Paris, J. Geophys. Res.
456 Atmos., 118, 2041–2057, doi:10.1002/jgrd.50059, 2013.

457 Bréon, F. M., Broquet, G., Puygrenier, V., Chevallier, F., Xueref-Remy, I., Ramonet, M.,
458 Dieudonné, E., Lopez, M., Schmidt, M., Perrussel, O., and Ciais, P.: An attempt at estimating
459 Paris area CO_2 emissions from atmospheric concentration measurements, Atmos. Chem.
460 Phys., 15, 1707-1724, doi:10.5194/acp-15-1707-2015, 2015.

461 BIPM: Vocabulaire international de métrologie - Concepts fondamentaux et généraux et
462 termes associés (VIM, 3è édition), Tech. Rep. JCGM 200 :2012, available at
463 http://www.bipm. org/fr/publications/guides/vim.html (last access: November 2015), 2012.

464 Chevallier, F., Ciais P., Conway T. J., Aalto T., Anderson B. E., Bousquet P., Brunke E. G.,
465 Ciattaglia L., Esaki Y., Fröhlich M., Gomez A.J., Gomez-Pelaez A.J., Haszpra L., Krummel P.,
466 Langenfelds R., Leuenberger M., Machida T., Maignan F., Matsueda H., Morguí J. A., Mukai
467 H., Nakazawa T., Peylin P., Ramonet M., Rivier L., Sawa Y., Schmidt M., Steele P., Vay S. A.,
468 Vermeulen A. T., Wofsy S., Worthy D.: CO_2 surface fluxes at grid point scale estimated from a
469 global 21-year reanalysis of atmospheric measurements. J. Geophys. Res., 115, D21307,
470 doi:10.1029/2010JD013887, 2010.

471 Dolgorouky, C., Gros, V., Sarda-Esteve, R., Sinha, V., Williams, J., Marchand, N., Sauvage, S.,
472 Poulain, L., Sciare, J., and Bonsang, B.: Total OH reactivity measurements in Paris during the
473 2010 MEGAPOLI winter campaign, Atmos. Chem. Phys., 12, 9593-9612, doi:10.5194/acp-12-
474 9593-2012, 2012.

EEA 2014: Air quality in Europe – 2014 report, European Environment Agency, available at: http://www.eea.europa.eu/publications/air-quality-in-europe-2014 (last access: April 2015), doi: 10.2800/22847, 2014.

Gros, V., Gaimoz, C., Herrmann, F., Custer, T., Williams, J., Bonsang, B., Sauvage, S., Locoge, N., d'Argouges, O., Sarda-Esteve, R., and Sciare, J.: Volatile Organic Compounds sources in Paris in spring 2007. Part I: Qualitative analysis, Environ. Chem., 8, 74–90, doi:10.1071/en10068, 2011.

INSEE, La population légale en Île-de-France au 1er Janvier 2012, Insee Flash, n°1, Décembre 2014.

Lauvaux T., Miles N. L., Richardson S.J., Deng A., Stauffer D.R., Davis K. J., Jacobson G., Rella C., Calonder G.-P., and DeCola P. L.: Urban Emissions of CO_2 from Davos, Switzerland: The First Real-Time Monitoring System Using an Atmospheric Inversion Technique. J. Appl. Meteor. Climatol., 52, 2654–2668, doi: http://dx.doi.org/10.1175/JAMC-D-13-038.1, 2013.

Levin, I., and Karstens, U.: Inferring high-resolution fossil fuel CO2 records at continental sites from combined 14CO2 and CO observations, Tellus B, *59*(2), 245-250, 2007.

Lopez, M., Schmidt, M., Delmotte, M., Colomb, A., Gros, V., Janssen, C., Lehman, S. J., Mondelain, D., Perrussel, O., Ramonet, M., Xueref-Remy, I., and Bousquet, P.: CO, NO_x and $^{13}CO_2$ as tracers for fossil fuel CO_2: results from a pilot study in Paris during winter 2010, Atmos. Chem. Phys., 13, 7343–7358, doi:10.5194/acp-13-7343-2013, 2013.

Miller, J. B., S. J. Lehman, S. A. Montzka, C. Sweeney, B. R. Miller, C. Wolak, E. J. Dlugokencky, J. R. Southon, J. C. Turnbull, and P. P. Tans: Linking emissions of fossil fuel CO_2 and other anthropogenic trace gases using atmospheric $^{14}CO_2$, J. Geophys. Res., 117, D08302, doi:10.1029/2011JD017048, 2012.

Saide, P., Bocquet, M., Osses, A., and Gallardo, L. : Constraining surface emissions of air pollutants using inverse modelling: method intercomparison and a new two-step two-scale regularization approach, Tellus B, 63: 360–370. doi: 10.1111/j.1600-0889.2011.00529.x, 2011.

SETRA: Emissions routières de polluants atmosphériques : courbes et facteurs d'influence, available at: http://catalogue.setra.fr/ documents/Catalogueseta/0005/Dtrf-0005666/DT5666.pdf (last access: September 2015), 2009.

Touaty, M., and Bonsang, B.: Hydrocarbon emissions in a highway tunnel in the Paris area, Atmos. Environ., 34, 985-996, 2000.

Turnbull J.C., Sweeney C., Karion A., Newberger T., Lehman S.J., Tans P.P., Davis K.J., Lauvaux T., Miles N.L., Richardson S.J., Cambaliza MO, Shepson P.B., Gurney K., Patarasuk R. and Razlivanov I.: Toward quantification and source sector identification of fossil fuel CO_2

510 emissions from an urban area: Results from the INFLUX experiment, J. Geophys. Res.
511 Atmos., 120,292–312, doi:10.1002/2014JD022555, 2015.

512 Turnbull, J. C., Karion, A., Fischer, M. L., Faloona, I., Guilderson, T., Lehman, S. J., Miller, B. R.,
513 Miller, J. B., Montzka, S., Sherwood, T., Saripalli, S., Sweeney, C., and Tans, P. P.: Assessment
514 of fossil fuel carbon dioxide and other anthropogenic trace gas emissions from airborne
515 measurements over Sacramento, California in spring 2009, Atmos. Chem. Phys., 11, 705-721,
516 doi:10.5194/acp-11-705-2011, 2011.

517 UNEP 2013: The Emissions Gap Report 2013, United Nations Environment Programme
518 (UNEP), Nairobi, available at : http://www.unep.org/pdf/UNEPEmissionsGapReport2013.pdf
519 (last access: April 2015), 2013.

520 Vogel, F. R., S. Hammer, A. Steinhof, B. Kromer, and I. Levin, Implication of weekly and
521 diurnal ^{14}C calibration on hourly estimates of CO-based fossil fuel CO_2 at a moderately
522 polluted site in southwestern Germany, Tellus B, 62(5), 512–520, doi:10.1111/j.1600-
523 0889.2010.00477.x, 2010.

524 Vogel, F. R., Levin, I., & Worthy, D. E. : Implications for Deriving Regional Fossil Fuel CO2
525 Estimates from Atmospheric Observations in a Hot Spot of Nuclear Power Plant 14CO2
526 Emissions. *Radiocarbon*, *55*(2–3), 1556-1572, 2013.

527 Yoshida, H., Mønster, J., and Scheutz, C.: Plant-integrated measurement of greenhouse gas
528 emissions from a municipal wastewater treatment plant, Water Res., 61, 108–118,
529 doi:10.1016/j.watres.2014.05.014, 2014.

530 Yver-Kwok, C. E., Müller, D., Caldow, C., Lebègue, B., Mønster, J. G., Rella, C. W., Scheutz, C.,
531 Schmidt, M., Ramonet, M., Warneke, T., Broquet, G., and Ciais, P.: Methane emission
532 estimates using chamber and tracer release experiments for a municipal waste water
533 treatment plant, Atmos. Meas. Tech. Discuss., 8, 2957-2999, doi:10.5194/amtd-8-2957-2015,
534 2015.

535 Zhang X., and Schreifels J.: Continuous emission monitoring systems at power plants in
536 China: Improving SO_2 emission measurement, Energy Policy, Volume 39, Issue 11, November
537 2011, Pages 7432-7438, ISSN 0301-4215, doi:10.1016/j.enpol.2011.09.011, 2011.

538

539

	ΔCO_2	ΔCO	ΔAcetylene	ΔEthylene	ΔPropene	Δi-pentane	Δn-pentane	ΔEthane	ΔPropane
ΔCO_2	-	**5.55 (0.24)**	**24.82 (2.13)**	52.55 (3.87)	11.18 (2.51)	**13.57 (2.34)**	9.27 (0.97)	49.81 (5.10)	32.07 (2.92)
ΔCO		-	3.48 (0.28)	**5.47 (0.39)**	1.32 (0.08)	**2.18 (0.15)**	1.15 (0.11)	6.56 (0.59)	3.19 (0.30)
ΔAcetylene			-	1.09 (0.06)	0.21 (0.01)	0.28 (0.02)	0.17 (0.01)	0.75 (0.10)	0.48 (0.04)
ΔEthylene				-	0.11 (0.01)	**0.19 (0.01)**	0.10 (0.01)	0.57 (0.04)	0.35 (0.02)
ΔPropene					-	0.72 (0.04)	**0.36 (0.03)**	1.87 (0.20)	**1.13 (0.09)**
Δi-pentane						-	0.44 (0.01)	1.73 (0.11)	0.89 (0.06)
Δn-pentane							-	2.66 (0.21)	1.14 (0.08)
ΔEthane								-	0.20 (0.01)
ΔPropane									-

Table 1: Observed ratios between co-emitted species derived from our method for the Multi-CO_2 campaign. Numbers in brackets () correspond to 1 σ. The mole fraction ratio is reported in ppb/ppm for ΔCO/ ΔCO_2, all others to ΔCO_2 are reported in ppt/ppm. Those that do not include ΔCO_2 are reported in ppb/ppb. For readability, the diagonal (unity ratios) has been replaced by dashes (-). Ratios in bold mean that they are in a satisfactory agreement with the ones from the MEGAPOLI/CO_2-Megaparis campaign (less than 15% of difference).

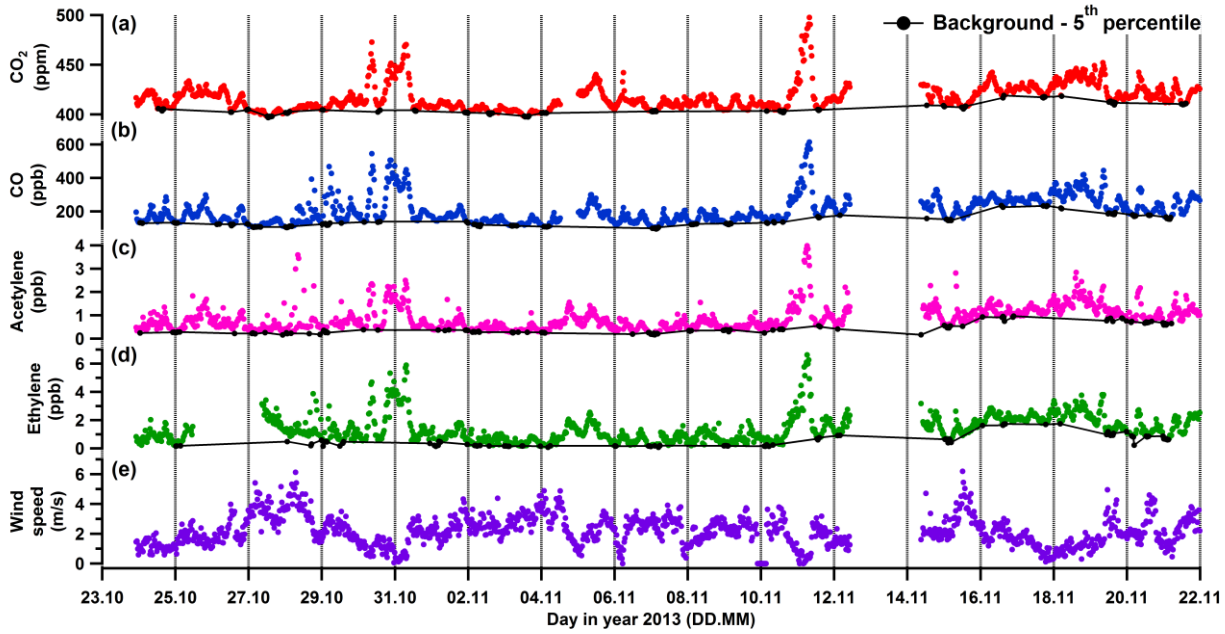

545

546 **Fig.1: (a-d)** Temporal variation of the mole fraction of selected compounds monitored during
547 the Multi-CO_2 campaign (30 minutes time step). The black lines represent the background
548 levels defined with the calculation of the 5th percentile (black disks). **(e)** Wind speed during
549 the campaign. Time is given in UTC.

550

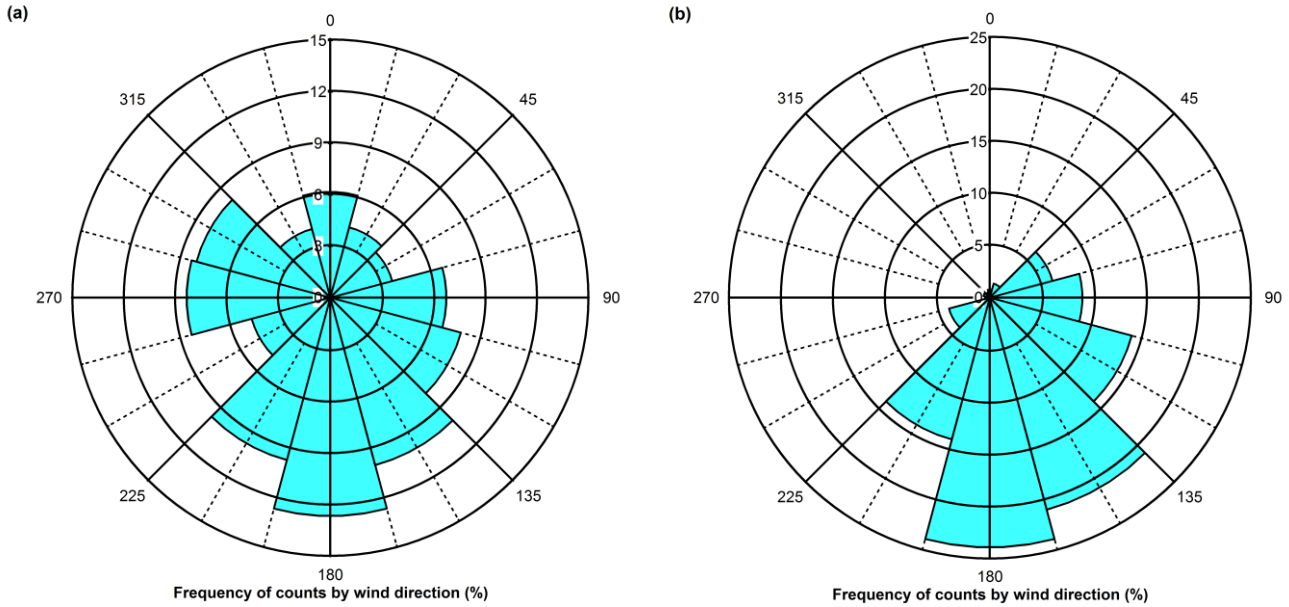

551

552 **Fig. 2:** Wind roses for two low wind speed situations. **(a)** Wind rose for 10-11 November
553 2013 (significant peak in mole fractions). **(b)** Wind rose for 18 November 2013 (no significant
554 peak in mole fractions). The percent scale is not the same for the two wind plots.

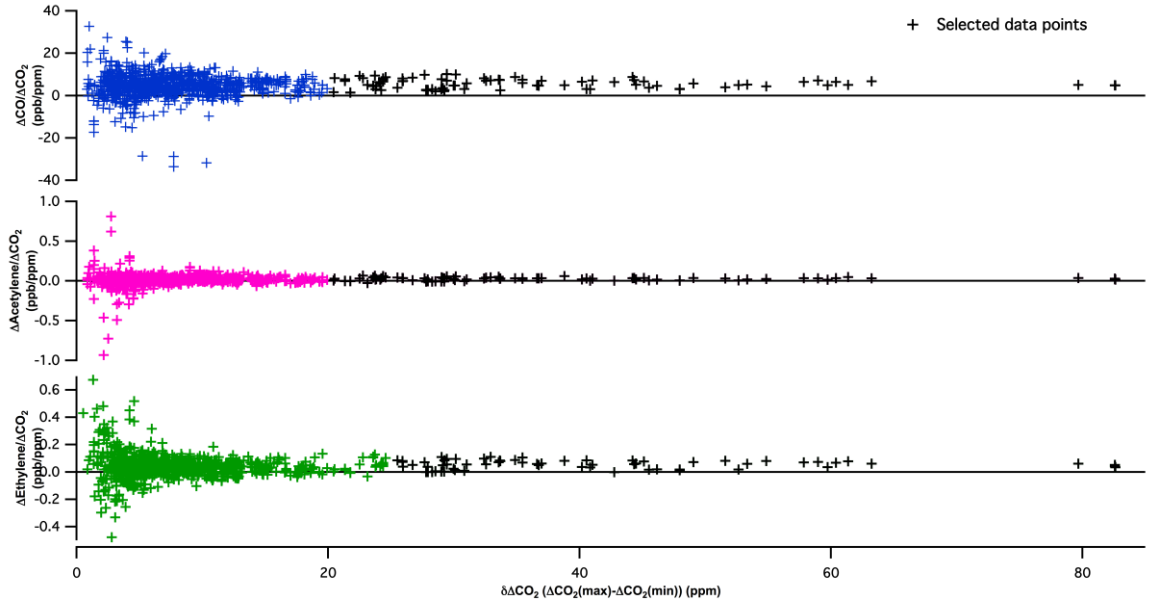

555

556 **Fig. 3:** Selected ratios to ΔCO_2 plotted versus the local CO_2 offset ($\delta\Delta CO_2$) from the
557 measurements acquired during the Multi-CO_2 campaign. Black data points were selected to
558 determine the equation of the horizontal asymptote using the criteria described in Section
559 3.3.2 (the used criteria depend on the considered species).

560

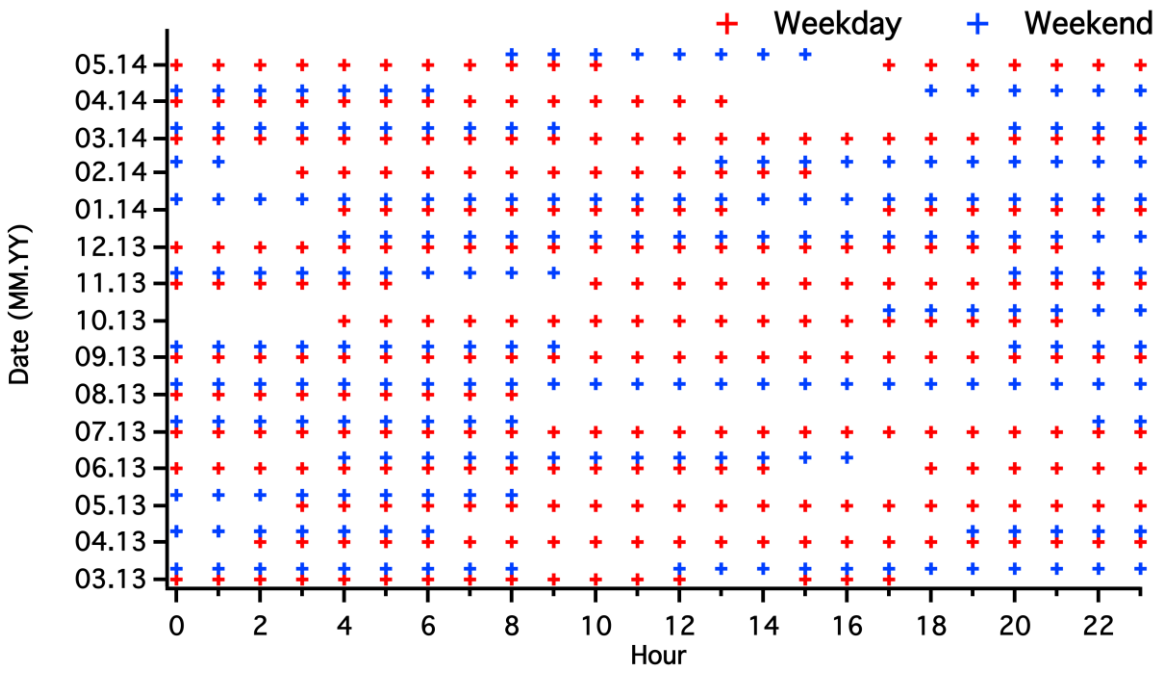

561

562 **Fig.4:** Days (weekdays in red crosses and weekends in blue crosses) and hour sampled per
563 month with our method.

564

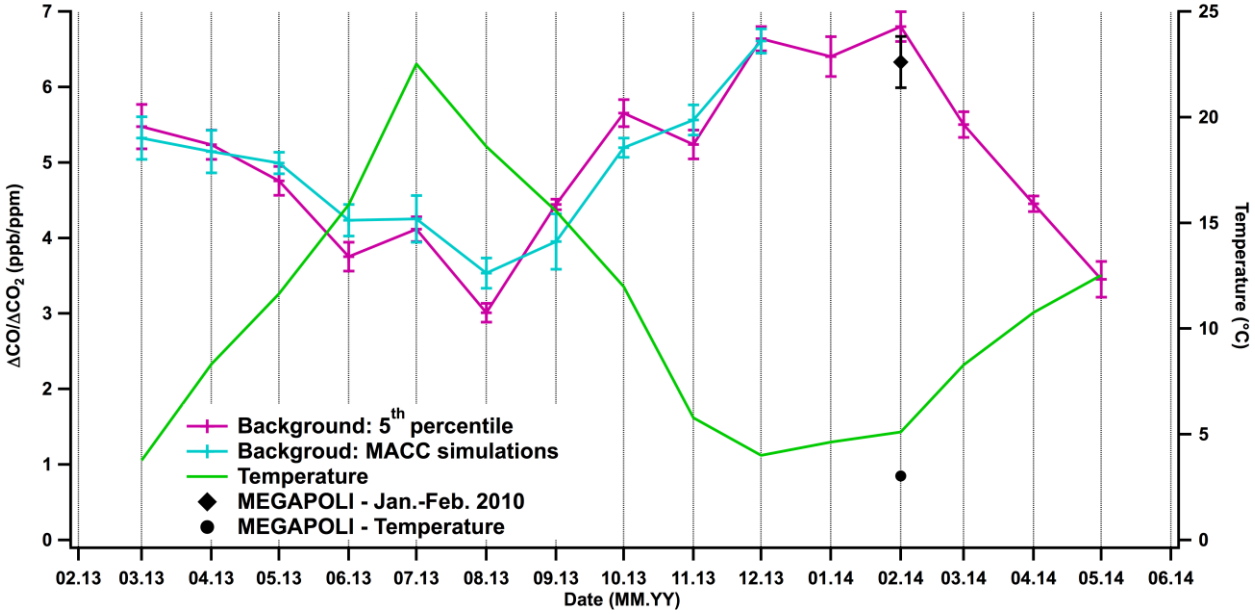

565

566 **Fig.5:** Monthly ΔCO to ΔCO_2 ratios in Paris. Results using background levels defined with the
567 5^{th} percentile are given in violet. The ones using the MACC simulations are in blue. Error bars
568 on the ratios correspond to 1σ. The ratio from the MEGAPOLI-CO_2-Megaparis campaign and
569 the corresponding average temperature are represented by a black disk. Temperature
570 corresponding to the selected data for the ratio calculation averaged by month is
571 represented in green as a proxy for season.

572